

Monte Carlo tools for studies of non-standard electroweak gauge boson interactions in multi-boson processes: A Snowmass White Paper

Celine Degrande,^{1,*} Oscar Eboli,^{2,†} Bastian Feigl,^{3,‡} Barbara Jäger,^{4,§} Wolfgang Kilian,^{5,¶} Olivier Mattelaer,^{6,**} Michael Rauch,^{7,††} Jürgen Reuter,^{8,‡‡} Marco Sekulla,^{5,§§} and Doreen Wackerroth (ed.)^{9,¶¶}

¹*Department of Physics, University of Illinois at Urbana Champaign, U.S.A*

²*Instituto de Física, Universidade de Sao Paulo, Sao Paulo - SP, Brazil*

³*Institute for Theoretical Physics, Karlsruhe Institute of Technology (KIT), Germany*

⁴*PRISMA Cluster of Excellence, Institut für Physik, Johannes-Gutenberg-Universität, Mainz, Germany*

⁵*Institut für Theoretische Physik I, Universität Siegen, Germany*

⁶*Department of Physics, University of Illinois at Urbana Champaign, U.S.A. and Center for Cosmology, Particle Physics and Phenomenology (CP3), Université Catholique de Louvain, Belgium*

⁷*Institute for Theoretical Physics, Karlsruhe Institute of Technology (KIT), Germany*

⁸*DESY Theory Group, Hamburg, Germany*

⁹*Department of Physics, University at Buffalo, The State University of New York, U.S.A.*

Abstract

In this Snowmass 2013 white paper, we review the effective field theory approach for studies of non-standard electroweak interactions in electroweak vector boson pair and triple production and vector boson scattering. We present an overview of the implementation of dimension six and eight operators in MadGraph5, VBFNLO, and WHIZARD, and provide relations between the coefficients of these higher dimensions operators used in these programs and in the anomalous couplings approach. We perform a tuned comparison of predictions for multi-boson processes including non-standard electroweak interactions with MadGraph5, VBFNLO, and WHIZARD. We discuss the role of higher-order corrections in these predictions using VBFNLO and a POWHEG BOX implementation of higher-order QCD corrections to $WWjj$ production. The purpose of this white paper is to collect useful tools for the study of non-standard EW physics at the LHC, compare them, and study the main physics issues in the relevant processes.

*cdegande@illinois.edu

†oeboli@gmail.com

‡bastian.feigl@kit.edu

§jaegerba@uni-mainz.de

¶kilian@physik.uni-siegen.de

**omatt@illinois.edu

††michael.rauch@kit.edu

‡‡juergen.reuter@desy.de

§§sekulla@physik.uni-siegen.de

¶¶dow@ubpheno.physics.buffalo.edu

Contents

II. Non-standard electroweak interactions	4
A. Effective field theory	4
B. Dimension-six operators for electroweak vector boson pair and triple production and scattering	4
C. Dimension-eight operators for genuine QGCs	6
1. Operators containing only $D_\mu\Phi$	6
2. Operators containing $D_\mu\Phi$ and two field strength tensors	7
3. Operators containing only field strength tensors	7
D. Comparison with the anomalous coupling approach and the LEP convention for aQGCs	8
E. Conventions for non-standard electroweak gauge boson interactions in different programs	9
1. Dimension-8 operators: VBFNLO and MadGraph5	9
2. Dimension-8 operators: WHIZARD	10
3. Dimension-6 operators: VBFNLO and MadGraph5	11
F. Discussion of unitarity bounds and usage of form factors	12
III. Predictions for multi-boson processes with non-standard couplings	14
A. MADGRAPH5	14
B. VBFNLO	15
C. The event generator WHIZARD	15
D. The Role of Higher-order Corrections	16
1. Vector-boson-fusion process W^+W^+jj with VBFNLO	16
2. Vector-boson-fusion process W^+W^+jj in the POWHEG BOX	17
3. Triboson process $W^+\gamma\gamma$ with VBFNLO	18
4. Electroweak corrections to triboson processes	20
IV. Comparison of predictions for multi-boson production with WHIZARD, VBFNLO and MADGRAPH	21
References	25
V. Summary	24
Acknowledgments	24

I. INTRODUCTION

After the LHC experiments have discovered a bosonic particle that is fully compatible with the Standard Model (SM) Higgs boson at the level of the electroweak (EW) precision observables, still the microscopic mechanism of EW symmetry breaking needs to be resolved. To prove that the SM is really the valid theory up to very high energy scales, one either needs to overconstrain the EW sector and test its structure at the level of next-to-leading order (NLO) corrections or find direct evidence for a possible dynamic explanation of the Higgs mechanism. One important ingredient is the structure of the selfinteractions of the Higgs field, which might give a hint on its underlying structure. For the scattering of a physical Higgs particle, measurements of these couplings are notoriously difficult, and while a measurement of the triple Higgs coupling seems feasible, the quartic coupling is hopeless. However, the Higgs field also contains the Goldstone bosons, i.e. the longitudinal modes of the EW gauge bosons. The scattering of the longitudinal modes is overlaid with the corresponding scattering of transversal EW gauge bosons from the non-Abelian structure of the EW gauge group. Phenomenologically, it is quite difficult to discriminate between them. Quartic interactions of EW gauge bosons can be studied in either triple boson production or vector boson scattering. There are two distinct cases: (i) where new physics can be directly probed, and (ii) where only indirect effects of new physics manifest themselves in the energy reach of the LHC (or its possible energy upgrade). There are many different models fitting the scenario (i) that are discussed in the BSM Snowmass white paper ¹. In all these cases, the assumption is that masses of those resonances are approximately in the 1-5 TeV range such that they can be directly probed at a 14 TeV machine. To cover this case in a mostly model-independent way, simplified models have been defined [1], where the issue of the unitarity of the longitudinal scattering amplitudes is carefully taken into account. In this document, the focus is on the more pessimistic scenario that new physics in the EW sector is out of the direct reach of the LHC or maybe even higher energy colliders. In that case one could integrate out new particles or resonances and one ends up with an effective field theory (EFT) with the SM as low-energy limit. While the translation between simplified new physics models in the EW sector to such an EFT are described in [1], there are also ambiguities for the low-energy EFT. This results from the choice of operator bases. In Section II the EFTs in different operator bases are discussed, and translations from one basis to another are defined. This should simplify the comparison between many different studies that have been performed for several past, present and future collider experiments. In Section III we collect the predictions from several studies for triboson production and vector boson scattering at the LHC, a 33 TeV energy upgrade as well as a 100 TeV high-energy hadron collider. In this section, also the codes used for these predictions are introduced and described in detail. One major purpose of this white paper is to collect useful tools for EW physics at the LHC, compare them and study the main physics issues in the relevant processes discussed above. These topics are described in Section IV. Finally, in Section V we summarize our findings.

¹ See www.snowmass2013.org for the report of the Snowmass 2013 working group *The Path Beyond the Standard Model*.

II. NON-STANDARD ELECTROWEAK INTERACTIONS

A. Effective field theory

If the energy scale of new physics is well above the energies reached in an experiment, the new degrees of freedom cannot be produced directly and new physics appears only as new interactions between the known particles. These new interactions are included in the Lagrangian as higher dimensional operators, which are invariant under the SM symmetries and suppressed by the new physics scale Λ ,

$$\mathcal{L}_{EFT} = \mathcal{L}_{SM} + \sum_{d>4} \sum_i \frac{\tilde{c}_i}{\Lambda^{d-4}} \mathcal{O}_i \quad (1)$$

where d is the dimension of the operators. In the limit $\Lambda \rightarrow \infty$, this Lagrangian reduces to the SM one. Since the coefficients of the higher dimensional operators, \tilde{c}_i , are fixed by the complete high-energy theory, any extension of the SM can be parametrized by this Lagrangian, where the \tilde{c}_i are kept as free parameters. Below the new physics scale, only the operators with lowest dimensions can give a large contribution and should therefore be kept. In particular, the SM contribution is expected to be larger than the new physics one. Once truncated, the Lagrangian becomes predictive even without fixing the coefficients and parametrizes any heavy new physics scenario. However, it should be kept in mind that this truncated Lagrangian is only valid below the new physics scale.

In the following, we will describe the EFT of new physics including dimension six and dimension eight operators that modify the interactions among electroweak gauge bosons:

$$\mathcal{L}_{EFT} = \mathcal{L}_{SM} + \sum_{i=WWW, WB, \Phi W, \Phi B} \frac{c_i}{\Lambda^2} \mathcal{O}_i + \sum_{j=1,2} \frac{f_{S,j}}{\Lambda^4} \mathcal{O}_{S,j} + \sum_{j=0,\dots,9} \frac{f_{T,j}}{\Lambda^4} \mathcal{O}_{T,j} + \sum_{j=0,\dots,7} \frac{f_{M,j}}{\Lambda^4} \mathcal{O}_{M,j} \quad (2)$$

B. Dimension-six operators for electroweak vector boson pair and triple production and scattering

If baryon and lepton numbers are conserved, only operators with even dimension can be constructed. Consequently, the largest new physics contribution is expected from dimension-six operators. Three CP conserving dimension-six operators,

$$\begin{aligned} \mathcal{O}_{WWW} &= \text{Tr}[W_{\mu\nu} W^{\nu\rho} W_{\rho}^{\mu}] \\ \mathcal{O}_W &= (D_{\mu}\Phi)^{\dagger} W^{\mu\nu} (D_{\nu}\Phi) \\ \mathcal{O}_B &= (D_{\mu}\Phi)^{\dagger} B^{\mu\nu} (D_{\nu}\Phi), \end{aligned} \quad (3)$$

and two CP violating dimension-six operators,

$$\begin{aligned} \mathcal{O}_{\tilde{W}WW} &= \text{Tr}[\tilde{W}_{\mu\nu} W^{\nu\rho} W_{\rho}^{\mu}] \\ \mathcal{O}_{\tilde{W}} &= (D_{\mu}\Phi)^{\dagger} \tilde{W}^{\mu\nu} (D_{\nu}\Phi), \end{aligned} \quad (4)$$

affect the triple and quartic gauge couplings. Here Φ denotes the Higgs doublet field and the covariant derivative for such a field with hypercharge $Y = 1/2$ is given by

$$D_{\mu} \equiv \partial_{\mu} + i \frac{g'}{2} B_{\mu} + i g W_{\mu}^i \frac{\tau^i}{2} \quad (5)$$

where $\tau^i, i = 1, 2, 3$ are the $SU(2)_I$ generators with $\text{Tr}[\tau^i \tau^j] = 2\delta^{ij}$. The field strength tensors of the $SU(2)_I$ (W_{μ}^i) and $U(1)_Y$ (B_{μ}) gauge fields read

$$\begin{aligned} W_{\mu\nu} &= \frac{i}{2} g \tau^i (\partial_{\mu} W_{\nu}^i - \partial_{\nu} W_{\mu}^i + g \epsilon_{ijk} W_{\mu}^j W_{\nu}^k) \\ B_{\mu\nu} &= \frac{i}{2} g' (\partial_{\mu} B_{\nu} - \partial_{\nu} B_{\mu}). \end{aligned} \quad (6)$$

Like in the SM, TGCs and QGCs from dimension-six operators are completely related to guarantee gauge invariance. In addition, three CP-conserving operators

$$\begin{aligned}\mathcal{O}_{\Phi d} &= \partial_\mu (\Phi^\dagger \Phi) \partial^\mu (\Phi^\dagger \Phi) \\ \mathcal{O}_{\Phi W} &= (\Phi^\dagger \Phi) \text{Tr}[W^{\mu\nu} W_{\mu\nu}] \\ \mathcal{O}_{\Phi B} &= (\Phi^\dagger \Phi) B^{\mu\nu} B_{\mu\nu}\end{aligned}\quad (7)$$

and two CP-violating dimension-six operators

$$\begin{aligned}\mathcal{O}_{\tilde{W}W} &= \Phi^\dagger \tilde{W}_{\mu\nu} W^{\mu\nu} \Phi \\ \mathcal{O}_{\tilde{B}B} &= \Phi^\dagger \tilde{B}_{\mu\nu} B^{\mu\nu} \Phi\end{aligned}\quad (8)$$

modify the coupling of the Higgs to the weak gauge bosons and therefore the four-gauge-boson amplitudes. The list of vertices relevant to three- and four-gauge-boson amplitudes of each operator is displayed in Tab. I. We have neglected the operators affecting the couplings of the bosons to fermions as they can be

	ZWW	AWW	HWW	HZZ	HZA	HAA	WWWW	ZZWW	ZAWW	AAWW
\mathcal{O}_{WWW}	X	X					X	X	X	X
\mathcal{O}_W	X	X	X	X	X		X	X	X	
\mathcal{O}_B	X	X		X	X					
$\mathcal{O}_{\Phi d}$			X	X						
$\mathcal{O}_{\Phi W}$			X	X	X	X				
$\mathcal{O}_{\Phi B}$				X	X	X				
$\mathcal{O}_{\tilde{W}WW}$	X	X					X	X	X	X
$\mathcal{O}_{\tilde{W}}$	X	X	X	X	X					
$\mathcal{O}_{\tilde{W}W}$			X	X	X	X				
$\mathcal{O}_{\tilde{B}B}$				X	X	X				

TABLE I: The vertices induced by each operator are marked with X in the corresponding column. The vertices that are not relevant for three- and four-gauge-boson amplitudes have been omitted.

measured in other processes such as Z decay. This is a minimal set of independent dimension-six operators relevant to amplitudes involving vertices of three and four electroweak gauge bosons. Additional dimension-six operators invariant under SM symmetries can be constructed but they can be shown to be equivalent to a linear combination of the previous operators by using equations of motion. Consequently, the choice of basis of operators is not unique and other choices than the one presented here can be found in the literature. For example, the operators $Q_{\Phi D}$ and $Q_{\Phi WB}$ in Ref. [2] have been replaced in this paper by \mathcal{O}_W and \mathcal{O}_B . Our basis avoids the otherwise necessary redefinition of the masses of the gauge bosons and the mixing of the neutral vector bosons. The operator $\mathcal{O}_{\Phi d}$ does not contain any gauge boson since $\Phi^\dagger \Phi$ is a singlet under all the SM gauge groups. However, it contributes to the Higgs field's kinetic term after Φ has been replaced by its value in the unitary gauge, i.e. with

$$\Phi = \left(0, \frac{v+h}{\sqrt{2}}\right)^T \quad (9)$$

one finds

$$\mathcal{O}_{\Phi d} \ni v^2 \partial_\mu h \partial^\mu h, \quad (10)$$

and it requires a renormalization of the Higgs field,

$$h \rightarrow h \left(1 - \frac{c_{\Phi d}}{\Lambda^2} v^2\right), \quad (11)$$

in the full Lagrangian. The Higgs couplings to all particles including the electroweak gauge bosons are consequently multiplied by the same factor. $\mathcal{O}_{\Phi W}$ and $\mathcal{O}_{\Phi B}$ modify the kinetic term of the gauge bosons

after the Higgs doublet has been replaced by its vacuum expectation value (v). Those two operators require then a renormalization of the gauge fields and the gauge couplings. As a matter of fact, their part proportional to v^2 is entirely absorbed by those redefinitions and can therefore be removed directly in the definition of the operators, i.e.

$$\begin{aligned}\mathcal{O}_{\Phi W} &= (\Phi^\dagger \Phi - v^2) \text{Tr}[W^{\mu\nu} W_{\mu\nu}] \\ \mathcal{O}_{\Phi B} &= (\Phi^\dagger \Phi - v^2) B^{\mu\nu} B_{\mu\nu}\end{aligned}\tag{12}$$

It is now clear that those operators affect only the vertices with one or two Higgs boson and not the TGCs or the QGCs.

C. Dimension-eight operators for genuine QGCs

As can be seen in Table I, the dimension–six operators giving rise to QGCs also exhibit TGCs. In order to separate the effects of the QGCs we shall consider effective operators that lead to QGCs without a TGC associated to them. Moreover, not all possible QGCs are generated by dimension–six operators, for instance, these operators do not give rise to quartic couplings among the neutral gauge bosons². The lowest dimension operator that leads to quartic interactions but does not exhibit two or three weak gauge boson vertices is of dimension eight³. The counting is straight forward: we can get a weak boson field either from the covariant derivative (D_μ of Eq. 5) of Φ or from the field strength tensor of Eq. 6. In either case, the vector field is accompanied by v (after using Eq. 9) or a derivative ∂_μ . Therefore, genuine quartic vertices are of dimension 8 or higher.

The idea behind using dimension–eight operators for QGCs is that the anomalous QGCs are to be considered as a straw man to evaluate the LHC potential to study these couplings, without having any theoretical prejudice about their size. There are three classes of genuine QGC operators [4]:

1. Operators containing only $D_\mu \Phi$

This class contains two independent operators, *i.e.*

$$\mathcal{O}_{S,0} = \left[(D_\mu \Phi)^\dagger D_\nu \Phi \right] \times \left[(D^\mu \Phi)^\dagger D^\nu \Phi \right], \tag{13}$$

$$\mathcal{O}_{S,1} = \left[(D_\mu \Phi)^\dagger D^\mu \Phi \right] \times \left[(D_\nu \Phi)^\dagger D^\nu \Phi \right], \tag{14}$$

where the Higgs covariant derivative is given by the expression in Eq. 5. These operators can be generated when we integrate out a spin–one resonance that couples to gauge–boson pairs with

$$\frac{f_{S,0}}{\Lambda^4} = -\frac{f_{S,1}}{\Lambda^4} = \frac{12\pi}{M_\rho^4} \frac{\Gamma_\rho}{M_\rho}, \tag{15}$$

where M_ρ (Γ_ρ) is the mass (width) of the vector resonance [5].

The operators $\mathcal{O}_{S,0}$ and $\mathcal{O}_{S,1}$ contain quartic $W^+W^-W^+W^-$, W^+W^-ZZ and $ZZZZ$ interactions that do not depend on the gauge boson momenta; for a comparative table showing all QGCs induced by dimension–eight operators see Table II. In our framework, the QGCs are accompanied by vertices with more than 4 particles due to gauge invariance. In order to simply rescale the SM quartic couplings containing W^\pm and Z it is enough to choose $f_{S,0} = -f_{S,1} = f$ which leads to SM quartic couplings modified by a factor $(1 + fv^4/8)$, where v is the Higgs vacuum expectation value ($v \simeq 246$ GeV).

² Notice that the lowest order operators leading to neutral TGCs are also of dimension eight.

³ Effective operators possessing QCGs but no TGCs can be generated at tree level by new physics at a higher scale [3], in contrast with operators containing TGCs that are generated at loop level.

2. Operators containing $D_\mu\Phi$ and two field strength tensors

QGCs are also generated by considering two electroweak field strength tensors and two covariant derivatives of the Higgs doublet [4]:

$$\mathcal{O}_{M,0} = \text{Tr} [W_{\mu\nu}W^{\mu\nu}] \times [(D_\beta\Phi)^\dagger D^\beta\Phi] , \quad (16)$$

$$\mathcal{O}_{M,1} = \text{Tr} [W_{\mu\nu}W^{\nu\beta}] \times [(D_\beta\Phi)^\dagger D^\mu\Phi] , \quad (17)$$

$$\mathcal{O}_{M,2} = [B_{\mu\nu}B^{\mu\nu}] \times [(D_\beta\Phi)^\dagger D^\beta\Phi] , \quad (18)$$

$$\mathcal{O}_{M,3} = [B_{\mu\nu}B^{\nu\beta}] \times [(D_\beta\Phi)^\dagger D^\mu\Phi] , \quad (19)$$

$$\mathcal{O}_{M,4} = [(D_\mu\Phi)^\dagger W_{\beta\nu}D^\mu\Phi] \times B^{\beta\nu} , \quad (20)$$

$$\mathcal{O}_{M,5} = [(D_\mu\Phi)^\dagger W_{\beta\nu}D^\nu\Phi] \times B^{\beta\mu} , \quad (21)$$

$$\mathcal{O}_{M,6} = [(D_\mu\Phi)^\dagger W_{\beta\nu}W^{\beta\nu}D^\mu\Phi] , \quad (22)$$

$$\mathcal{O}_{M,7} = [(D_\mu\Phi)^\dagger W_{\beta\nu}W^{\beta\mu}D^\nu\Phi] , \quad (23)$$

where the field strengths $W_{\mu\nu}$ and $B_{\mu\nu}$ have been defined above in Eq. (6). In this class of effective operators the quartic gauge-boson interactions depend upon the momenta of the vector bosons due to the presence of the field strength in their definitions. Therefore, the Lorentz structure of these operators can not be reduced to the SM one. The complete list of quartic vertices modified by these operators can be found in Table II.

3. Operators containing only field strength tensors

The following operators containing four field strength tensors also lead to quartic anomalous couplings:

$$\mathcal{O}_{T,0} = \text{Tr} [W_{\mu\nu}W^{\mu\nu}] \times \text{Tr} [W_{\alpha\beta}W^{\alpha\beta}] , \quad (24)$$

$$\mathcal{O}_{T,1} = \text{Tr} [W_{\alpha\nu}W^{\mu\beta}] \times \text{Tr} [W_{\mu\beta}W^{\alpha\nu}] , \quad (25)$$

$$\mathcal{O}_{T,2} = \text{Tr} [W_{\alpha\mu}W^{\mu\beta}] \times \text{Tr} [W_{\beta\nu}W^{\nu\alpha}] , \quad (26)$$

$$\mathcal{O}_{T,5} = \text{Tr} [W_{\mu\nu}W^{\mu\nu}] \times B_{\alpha\beta}B^{\alpha\beta} , \quad (27)$$

$$\mathcal{O}_{T,6} = \text{Tr} [W_{\alpha\nu}W^{\mu\beta}] \times B_{\mu\beta}B^{\alpha\nu} , \quad (28)$$

$$\mathcal{O}_{T,7} = \text{Tr} [W_{\alpha\mu}W^{\mu\beta}] \times B_{\beta\nu}B^{\nu\alpha} , \quad (29)$$

$$\mathcal{O}_{T,8} = B_{\mu\nu}B^{\mu\nu}B_{\alpha\beta}B^{\alpha\beta} \quad (30)$$

$$\mathcal{O}_{T,9} = B_{\alpha\mu}B^{\mu\beta}B_{\beta\nu}B^{\nu\alpha} . \quad (31)$$

It is interesting to note that the two last operators $\mathcal{O}_{T,8}$ and $\mathcal{O}_{T,9}$ give rise to QGCs containing only the neutral electroweak gauge bosons.

Previous analyses [6–8] of the LHC potential to study QGCs were based on the non-linear realization of the gauge symmetry, *i.e.* using chiral Lagrangians as for instance implemented in WHIZARD. The relation between the above framework and chiral Lagrangians can be found in Section II E 2.

	WWWW	WWZZ	ZZZZ	WWAZ	WWAA	ZZZA	ZZAA	ZAAA	AAAA
$\mathcal{O}_{S,0}, \mathcal{O}_{S,1}$	X	X	X						
$\mathcal{O}_{M,0}, \mathcal{O}_{M,1}, \mathcal{O}_{M,6}, \mathcal{O}_{M,7}$	X	X	X	X	X	X	X		
$\mathcal{O}_{M,2}, \mathcal{O}_{M,3}, \mathcal{O}_{M,4}, \mathcal{O}_{M,5}$		X	X	X	X	X	X		
$\mathcal{O}_{T,0}, \mathcal{O}_{T,1}, \mathcal{O}_{T,2}$	X	X	X	X	X	X	X	X	X
$\mathcal{O}_{T,5}, \mathcal{O}_{T,6}, \mathcal{O}_{T,7}$		X	X	X	X	X	X	X	X
$\mathcal{O}_{T,8}, \mathcal{O}_{T,9}$			X			X	X	X	X

TABLE II: Quartic vertices modified by each dimension-8 operator are marked with X.

D. Comparison with the anomalous coupling approach and the LEP convention for aQGCs

The anomalous couplings approach is based on the Lagrangian [9]

$$\begin{aligned}
\mathcal{L} = & ig_{WWV} \left(g_1^V (W_{\mu\nu}^+ W^{-\mu} - W^{+\mu} W_{\mu\nu}^-) V^\nu + \kappa_V W_\mu^+ W_\nu^- V^{\mu\nu} + \frac{\lambda_V}{M_W^2} W_\mu^{\nu+} W_\nu^{-\rho} V_\rho^\mu \right. \\
& + ig_4^V W_\mu^+ W_\nu^- (\partial^\mu V^\nu + \partial^\nu V^\mu) - ig_5^V \epsilon^{\mu\nu\rho\sigma} (W_\mu^+ \partial_\rho W_\nu^- - \partial_\rho W_\mu^+ W_\nu^-) V_\sigma \\
& \left. + \tilde{\kappa}_V W_\mu^+ W_\nu^- \tilde{V}^{\mu\nu} + \frac{\tilde{\lambda}_V}{m_W^2} W_\mu^{\nu+} W_\nu^{-\rho} \tilde{V}_\rho^\mu \right), \tag{32}
\end{aligned}$$

where $V = \gamma, Z$; $W_{\mu\nu}^\pm = \partial_\mu W_\nu^\pm - \partial_\nu W_\mu^\pm$, $V_{\mu\nu} = \partial_\mu V_\nu - \partial_\nu V_\mu$, $g_{WW\gamma} = -e$ and $g_{WWZ} = -e \cot \theta_W$. The first three terms of Eq. 32 are C and P invariant while the remaining four terms violate C and/or P . Electromagnetic gauge invariance requires that $g_1^\gamma = 1$ and $g_4^\gamma = g_5^\gamma = 0$. Finally there are five independent C - and P -conserving parameters: $g_1^Z, \kappa_\gamma, \kappa_Z, \lambda_\gamma, \lambda_Z$; and six C and/or P violating parameters: $g_4^Z, g_5^Z, \tilde{\kappa}_\gamma, \tilde{\kappa}_Z, \tilde{\lambda}_\gamma, \tilde{\lambda}_Z$. This Lagrangian is not the most generic one as extra derivatives can be added in all the operators. Furthermore, there is no reason to remove those extra terms since they are not suppressed by Λ but by M_W .

The effective field theory approach described in the previous section allows one to calculate those parameters in terms of the coefficients of the five dimension-six operators relevant for TGCs, i.e. in terms of the EFT coefficients $c_{WWW}, c_W, c_B, c_{\bar{W}WW}$ and $c_{\bar{W}}$. One finds for the anomalous TGC parameters [10, 11]:

$$g_1^Z = 1 + c_W \frac{m_Z^2}{2\Lambda^2} \tag{33}$$

$$\kappa_\gamma = 1 + (c_W + c_B) \frac{m_W^2}{2\Lambda^2} \tag{34}$$

$$\kappa_Z = 1 + (c_W - c_B \tan^2 \theta_W) \frac{m_W^2}{2\Lambda^2} \tag{35}$$

$$\lambda_\gamma = \lambda_Z = c_{WWW} \frac{3g^2 m_W^2}{2\Lambda^2} \tag{36}$$

$$g_4^V = g_5^V = 0 \tag{37}$$

$$\tilde{\kappa}_\gamma = c_{\bar{W}} \frac{m_W^2}{2\Lambda^2} \tag{38}$$

$$\tilde{\kappa}_Z = -c_{\bar{W}} \tan^2 \theta_W \frac{m_W^2}{2\Lambda^2} \tag{39}$$

$$\tilde{\lambda}_\gamma = \tilde{\lambda}_Z = c_{\bar{W}WW} \frac{3g^2 m_W^2}{2\Lambda^2} \tag{40}$$

Defining $\Delta g_1^Z = g_1^Z - 1$, $\Delta \kappa_{\gamma,Z} = \kappa_{\gamma,Z} - 1$, the relation [10]

$$\Delta g_1^Z = \Delta \kappa_Z + \tan^2 \theta_W \Delta \kappa_\gamma \tag{41}$$

and the relation $\lambda_\gamma = \lambda_Z$ reduce the five C and P conserving parameters down to three. For the C and/or P violating parameters, the relation

$$0 = \tilde{\kappa}_Z + \tan^2 \theta_W \tilde{\kappa}_\gamma \quad (42)$$

and the relations $\tilde{\lambda}_\gamma = \tilde{\lambda}_Z$ and $g_4^Z = g_5^Z = 0$ reduce the six C and/or P violating parameters down to just two.

The Lagrangian of Eq. 32 is not $SU(2)_L$ gauge invariant even after imposing those relations because the quartic and higher multiplicity couplings are not included. Furthermore, gauge invariance requires also several relations between vertices with different number of particles. Therefore, the anomalous coupling Lagrangian cannot be used for four-gauge-boson amplitudes. The quartic couplings involving two photons have been parametrized in a similar way. However, the parametrization is not generic enough and does not include the contributions from the dimension-six operators.

The LEP2 constraints on the vertices $\gamma\gamma W^+W^-$ and $\gamma\gamma ZZ$ [12] described in terms of anomalous couplings a_0/Λ^2 and a_c/Λ^2 can be translated into bounds on $f_{M,0} - f_{M,7}$. In Ref. [13] (see also Refs [14, 15]), genuine anomalous quartic couplings involving two photons have been introduced as follows:

$$\begin{aligned} \mathcal{L}_0 &= -\frac{e^2}{16\pi\Lambda^2} a_0 F_{\mu\nu} F^{\mu\nu} \vec{W}^\alpha \vec{W}_\alpha \\ \mathcal{L}_c &= -\frac{e^2}{16\pi\Lambda^2} a_c F_{\mu\alpha} F^{\mu\beta} \vec{W}^\alpha \vec{W}_\beta \end{aligned} \quad (43)$$

with

$$\begin{aligned} F^{\mu\nu} &= \partial^\mu A^\nu - \partial^\nu A^\mu \\ \vec{W}_\mu &= \begin{pmatrix} \frac{1}{\sqrt{2}}(W_\mu^+ + W_\mu^-) \\ \frac{i}{\sqrt{2}}(W_\mu^+ - W_\mu^-) \\ \frac{Z_\mu}{\cos\theta_w} \end{pmatrix} \end{aligned} \quad (44)$$

where A_μ and W_μ^\pm, Z_μ denote the photon and weak fields, respectively. Thus, using the conventions of Eq. 6 for the fields in the operators $\mathcal{O}_{M,i}$, and Eq. 44 for the fields in the operators $\mathcal{L}_0/\mathcal{L}_c$, the following relations for the $WW\gamma\gamma$ (upper sign) and $ZZ\gamma\gamma$ (lower sign) vertices can be derived:

$$\frac{f_{M,0}}{\Lambda^4} = \frac{a_0}{\Lambda^2} \frac{1}{g^2 v^2} \quad \text{and} \quad \frac{f_{M,1}}{\Lambda^4} = -\frac{a_c}{\Lambda^2} \frac{1}{g^2 v^2} \quad (45)$$

$$\frac{f_{M,2}}{\Lambda^4} = \frac{a_0}{\Lambda^2} \frac{2}{g^2 v^2} \quad \text{and} \quad \frac{f_{M,3}}{\Lambda^4} = -\frac{a_c}{\Lambda^2} \frac{2}{g^2 v^2} \quad (46)$$

$$\frac{f_{M,4}}{\Lambda^4} = \pm \frac{a_0}{\Lambda^2} \frac{1}{g^2 v^2} \quad \text{and} \quad \frac{f_{M,5}}{\Lambda^4} = \pm \frac{a_c}{\Lambda^2} \frac{2}{g^2 v^2} \quad (47)$$

$$\frac{f_{M,6}}{\Lambda^4} = \frac{a_0}{\Lambda^2} \frac{2}{g^2 v^2} \quad \text{and} \quad \frac{f_{M,7}}{\Lambda^4} = \frac{a_c}{\Lambda^2} \frac{2}{g^2 v^2} . \quad (48)$$

E. Conventions for non-standard electroweak gauge boson interactions in different programs

1. Dimension-8 operators: VBFNLO and MadGraph5

The convention for the dimension-8-operators in VBFNLO is the same as described in Section II C, and the coefficients f_i/Λ^4 set in the input file are the ones that multiply the operators of Section II C. However, the MadGraph5 implementation by means of a UFO file [16] uses expressions for the field strengths which

are slightly different than the ones from Eq. 6:

$$\begin{aligned}\widehat{W}_{\mu\nu} &= \frac{1}{2}\tau^i(\partial_\mu W_\nu^i - \partial_\nu W_\mu^i + g\epsilon_{ijk}W_\mu^j W_\nu^k) = \frac{1}{ig}W_{\mu\nu} \\ \widehat{B}_{\mu\nu} &= (\partial_\mu B_\nu - \partial_\nu B_\mu) = \frac{2}{ig'}B_{\mu\nu}\end{aligned}\tag{49}$$

The resulting changes can be absorbed in a redefinition of the operator coefficients:

$$f_{S,0,1} = f_{S,0,1}^{\text{VBFNLO}} = f_{S,0,1}^{\text{MG5}}\tag{50}$$

$$f_{M,0,1} = f_{M,0,1}^{\text{VBFNLO}} = -\frac{1}{g^2} \cdot f_{M,0,1}^{\text{MG5}}\tag{51}$$

$$f_{M,2,3} = f_{M,2,3}^{\text{VBFNLO}} = -\frac{4}{g'^2} \cdot f_{M,2,3}^{\text{MG5}}\tag{52}$$

$$f_{M,4,5} = f_{M,4,5}^{\text{VBFNLO}} = -\frac{2}{gg'} \cdot f_{M,4,5}^{\text{MG5}}\tag{53}$$

$$f_{M,6,7} = f_{M,6,7}^{\text{VBFNLO}} = -\frac{1}{g^2} \cdot f_{M,6,7}^{\text{MG5}}\tag{54}$$

$$f_{T,0,1,2} = f_{T,0,1,2}^{\text{VBFNLO}} = \frac{1}{g^4} \cdot f_{T,0,1,2}^{\text{MG5}}\tag{55}$$

$$f_{T,5,6,7} = f_{T,5,6,7}^{\text{VBFNLO}} = \frac{4}{g^2 g'^2} \cdot f_{T,5,6,7}^{\text{MG5}}\tag{56}$$

$$f_{T,8,9} = f_{T,8,9}^{\text{VBFNLO}} = \frac{16}{g'^4} \cdot f_{T,8,9}^{\text{MG5}}\tag{57}$$

2. Dimension-8 operators: WHIZARD

As WHIZARD uses different anomalous couplings operators than the ones described in Section II C, assuming a different symmetry group [17], a conversion is in general not possible. However, a vertex-specific conversion exists for the operators $\mathcal{O}_{S,0}$ and $\mathcal{O}_{S,1}$ to their corresponding operators

$$\mathcal{L}_4^{(4)} = \alpha_4 [\text{Tr}(V_\mu V_\nu)]^2\tag{58}$$

$$\mathcal{L}_5^{(4)} = \alpha_5 [\text{Tr}(V_\mu V^\mu)]^2, \quad \text{with } V_\mu = (D_\mu \Sigma) \Sigma^\dagger.\tag{59}$$

The conversion reads:

- for the WWWW-Vertex:

$$\alpha_4 = \frac{f_{S,0}}{\Lambda^4} \frac{v^4}{8}\tag{60}$$

$$\alpha_4 + 2 \cdot \alpha_5 = \frac{f_{S,1}}{\Lambda^4} \frac{v^4}{8}\tag{61}$$

- for the WWZZ-Vertex:

$$\alpha_4 = \frac{f_{S,0}}{\Lambda^4} \frac{v^4}{16}\tag{62}$$

$$\alpha_5 = \frac{f_{S,1}}{\Lambda^4} \frac{v^4}{16}\tag{63}$$

- for the ZZZZ-Vertex:

$$\alpha_4 + \alpha_5 = \left(\frac{f_{S,0}}{\Lambda^4} + \frac{f_{S,1}}{\Lambda^4} \right) \frac{v^4}{16}\tag{64}$$

3. Dimension-6 operators: VBFNLO and MadGraph5

The MadGraph model EWdim6 has been generated from FeynRules and contains the operators from Eqs. 3, 4 and 7, with the exception of $\mathcal{O}_{\tilde{W}W}$, $\mathcal{O}_{\tilde{B}B}$ and $\mathcal{O}_{D\tilde{W}}$ ⁴. The names of the coefficients is displayed in Tab. III. All the coefficients include the $1/\Lambda^2$ as reminded by the "L2" at the end of the names and are in TeV^{-2} . The model also has a new coupling order NP counting the power of $1/\Lambda$. Consequently, each vertex from the dimension-six operators has $NP=2$.

c_{WW}/Λ^2	CWWL2
c_W/Λ^2	CWL2
c_B/Λ^2	CBL2
$c_{\tilde{W}WW}/\Lambda^2$	CPWWL2
$c_{\tilde{W}}/\Lambda^2$	CPWL2
$c_{\Phi d}/\Lambda^2$	CphidL2
$c_{\Phi W}/\Lambda^2$	CphiWL2
$c_{\Phi B}/\Lambda^2$	CphiBL2

TABLE III: Names of the couplings of the dimension-six operators present in the EWdim6 model of MadGraph5.

The operators from Eqs. 3 and 4 in Section IIB are directly available in VBFNLO. From Eq. 7 the operators $\mathcal{O}_{\tilde{W}W}$, $\mathcal{O}_{\tilde{B}B}$ and $\mathcal{O}_{\Phi B}$ are available as well ($\mathcal{O}_{\Phi B}$ is called \mathcal{O}_{BB} within VBFNLO). Additionally, the operator

$$\mathcal{O}_{WW} = \Phi^\dagger W_{\mu\nu} W^{\mu\nu} \Phi \quad (65)$$

from VBFNLO can be related to the operator $\mathcal{O}_{\Phi W}$ by choosing the coefficient as

$$c_{WW} = 2 \cdot c_{\Phi W} \quad (66)$$

In addition to those operators, VBFNLO also provides the following CP-odd operators:

$$\begin{aligned} \mathcal{O}_{\tilde{B}} &= (D_\mu \Phi)^\dagger \tilde{B}^{\mu\nu} (D_\nu \Phi) \\ \mathcal{O}_{B\tilde{W}} &= \Phi^\dagger B_{\mu\nu} \tilde{W}^{\mu\nu} \Phi \\ \mathcal{O}_{D\tilde{W}} &= \text{Tr} \left([D_\mu, \tilde{W}_{\nu\rho}] [D^\mu, \tilde{W}^{\nu\rho}] \right). \end{aligned} \quad (67)$$

However, only 4 of the 7 CP-odd operators are linearly independent, so the additional operators can be expressed in terms of the operators of Eqs. 4 and 8 as follows:

$$\begin{aligned} \mathcal{O}_{\tilde{B}} &= \mathcal{O}_{\tilde{W}} + \frac{1}{2} \mathcal{O}_{\tilde{W}W} - \frac{1}{2} \mathcal{O}_{\tilde{B}B} \\ \mathcal{O}_{B\tilde{W}} &= -2 \mathcal{O}_{\tilde{W}} - \mathcal{O}_{\tilde{W}W} \\ \mathcal{O}_{D\tilde{W}} &= -4 \mathcal{O}_{\tilde{W}WW}. \end{aligned} \quad (68)$$

The CP-conserving anomalous couplings implementation is also available in VBFNLO with the parameters Δg_1^Z , $\Delta \kappa_Z$, $\Delta \kappa_\gamma$, and λ_γ , defined in Section IID.

⁴ We have neglected the CP violating operators with the dual strength tensors affecting only the gauge boson Higgs couplings, since measuring CP violation in the four-weak-boson amplitude would be very challenging.

F. Discussion of unitarity bounds and usage of form factors

The effective field theory is valid only below the new physics scale Λ and no violation of unitarity occurs in this regime. In the regime where EFT is valid, the new physics contributions to a SM process, i.e. the interference of the SM amplitude with the higher-dimensional operators and the square of the new physics amplitudes, are suppressed by increasing powers of $1/\Lambda$,

$$|\mathcal{M}_{SM} + \mathcal{M}_{dim6} + \mathcal{M}_{dim8} + \dots|^2 = \underbrace{|\mathcal{M}_{SM}|^2}_{\Lambda^0} + \underbrace{2\Re(\mathcal{M}_{SM}\mathcal{M}_{dim6})}_{\Lambda^{-2}} + \underbrace{|\mathcal{M}_{dim6}|^2 + 2\Re(\mathcal{M}_{SM}\mathcal{M}_{dim8})}_{\Lambda^{-4}} + \dots \quad (69)$$

For illustration we show in Fig. 1 the invariant mass distribution of the W -pair, m_{WW} , produced at the 14 TeV LHC, with and without the contribution of the dimension six operator \mathcal{O}_{WWW} of Eq. 3. As can be seen on the l.h.s., the prediction for m_{WW} including \mathcal{O}_{WWW} is well below the unitarity bound [18] for this process in the relevant energy regime. However, as illustrated on the r.h.s., the contributions of this operator to the amplitude squared for $W_L W_T$ production reach similar magnitude at $m_{WW} \approx 1.3$ TeV and above this energy the $1/\Lambda^4$ suppressed term overtakes the $1/\Lambda^2$ suppressed contribution. Clearly, the $1/\Lambda$ expansion is only valid below this energy.

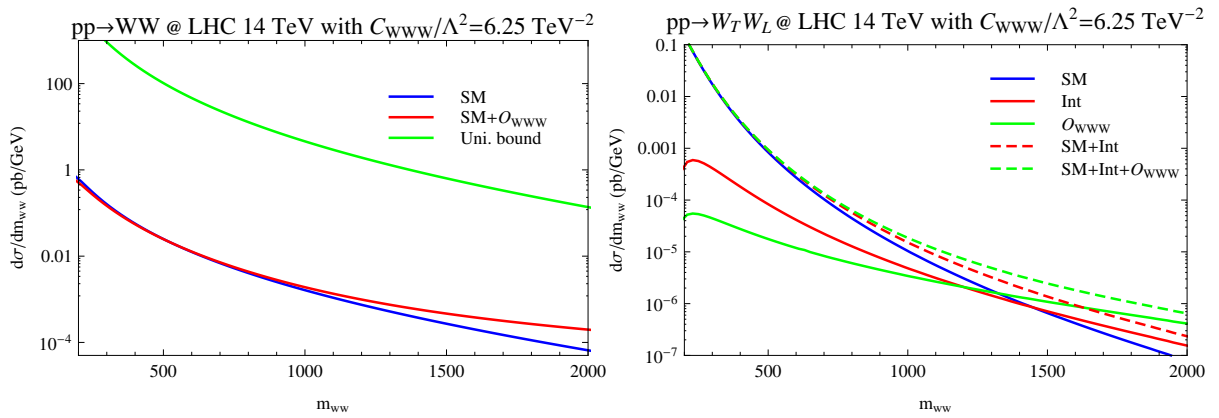


FIG. 1: m_{WW} distributions in W -pair production at the 14 TeV LHC are displayed on the l.h.s. for the SM (in blue) and for the SM plus the dimension six operator \mathcal{O}_{WWW} with $c_{WWW}/\Lambda^2 = 6.25$ TeV (in red). Also shown is the unitarity bound [18] (in green). The figure on the r.h.s. shows the m_{WW} distribution for the production of one longitudinally and one transversally polarized W boson, when considering the SM (solid blue line), only the interference between the SM and the dimension-six operator (solid red line), the sum of the two (dashed red line), only the square of the new physics amplitude (solid green line), and finally the total contribution from the SM and the dimension-six operator (dashed green line).

For dimension eight operators, the effect from unitarity violation typically sets in earlier due to the higher exponent in Λ in the denominator. Hence, the task to avoid unphysical contributions from regions where unitarity is violated becomes more important. In these regions the EFT expansion in terms of suppressed additional contributions to the SM part, our starting point, is no longer valid, as each order becomes similarly important.

In experimental searches one has to ensure that the sensitivity on anomalous gauge couplings is not driven by parameter regions where unitarity is violated. As nature will ensure unitarity conservation in the full model, such results would not be meaningful. Thereby, one can take advantage of the fact that only energies up to the center-of-mass energy of the collider are probed. For hadron colliders like the LHC, the steep fall-off of the parton distribution functions means that the effective probed energy range is even smaller, as the expected number of signal events will be smaller than one above a certain energy and therefore this region will not contribute. However, if the bound for unitarity violation is lower than that, some method to ensure that no sensitivity comes from this energy range needs to be employed. One possibility is to use

appropriate experimental cuts. However, often processes will contain neutrinos and so the full reconstruction of the partonic energy is not possible. Another option are form factors. These are introduced to model an energy-dependent cutoff, which in the full theory would be accomplished by new-physics states at the scale Λ , which have been integrated out in the EFT description. Various options are possible, for example a sharp cut-off of the higher-dimensional contributions at a fixed energy scale, or a dipole-like form factor as used in VBFNLO, that gives a smoother cut-off. The exact choice depends on the full model, so for an effective theory description all choices are equally well motivated from the theory side. The last possibility to ensure no unitarity violation happens is a unitarity projection, like the K -matrix method implemented in WHIZARD. There the amplitude A is moved onto the unitarity circle along a line connecting $\Re(A)$ and the imaginary unit i . Physically, this corresponds to introducing an infinitely heavy and wide resonance. This scheme maximizes the contributions from anomalous couplings while ensuring unitarity for all energies.

III. PREDICTIONS FOR MULTI-BOSON PROCESSES WITH NON-STANDARD COUPLINGS

A. MadGraph5

MADGRAPH5 [19] is a suite of programs related to the numerical evaluation of the matrix element [20–22]. In particular, the tool is able to compute the cross section and to generate events at leading order accuracy [23]. It also contains an interface to PYTHIA6 [24] to generate inclusive samples at LO+PS accuracy via the CKKW matching/merging scheme [25, 26]. Additionally, a public beta version (2.0.0beta4) of the code allows to perform the computation at next-to-leading order accuracy in QCD matched to a parton shower via the AMC@NLO module [27]. As in the LO mode, there is no predefined list of processes, AMC@NLO is able to generate fully automatically an optimized way to evaluate the matrix element and the associate phase space integration.

At leading order, the program has been designed to be fully model independent. In addition to its own model format, MADGRAPH5 contains an interface to support a model written in the UFO convention [28]. This model is by essence fully generic and not tied to any Monte Carlo generator. Unfortunately, MadGraph has some small limitation on the model that can be imported via this format. First, MADGRAPH5 does not support spin larger than 2. Secondly, the color module does not support representation 10 or higher, but includes the sextet and the support for the fully anti-symmetric color-structure. On the other hand, there are no limitations on the Lorentz structure allowed for a given interactions and in particular on the number of particles. Indeed MADGRAPH5 calls the ALOHA package [29] in order to create the helicity amplitude routine [30] that are needed for the efficient evaluation of the matrix element. As a small exception, MADGRAPH5 does not support multi-fermion interactions in presence of fermion-flow violation, but all other type of multi-fermion interactions are supported including the case of identical fermions. A recent extension of the UFO and ALOHA package [31] allows MADGRAPH5 to support user-defined propagators as well as form factors.

Writing a UFO model is obviously somewhat tedious, fortunately various packages allow to create models automatically for a large class of local theories. This format is currently supported by FEYNRULES [32, 33] and SARAH [34], and is planned to be supported by LANHEP [35] as well. An extension of the UFO model for next-to-leading accuracy is on its way as well as a FEYNRULES interface to create models automatically [36].

One key feature of MADGRAPH5 at leading order is that one can easily specify the decay chain structure associated to a production process. In such cases, MADGRAPH5 is able to generate events with up to 16 particles in the final state including full spin correlations and off-shell effects⁵. An alternative, which is especially useful at NLO, consists of generating the production process at parton-level without decay, and then using the MADSPIN package [37] to generate the decay also with full spin-correlations and off-shell effects.

MADGRAPH5 contains also a large class of options concerning the parton-level cuts and beam parametrizations. For example, it supports polarized beams and beamstrahlung, LHAPDF. Finally, the MADGRAPH5 interface is designed to be user friendly and contains a built-in tutorial to facilitate the apprentissage procedure and can install (and link) fully automatically a series of external codes (e.g., PYTHIA6 [24], MADANALYSIS [38], DELPHES [39]). With all those features, MADGRAPH5 is a very flexible tool which can describe efficiently and precisely a large class of phenomenological processes, and in the electroweak sector in particular. It is therefore often a tool of choice for the study of the physics potential of future accelerators.

⁵ Since such computations are stricto-sensu only valid in the narrow-width approximation, a customizable cut is added to forbid the decaying particles to be too far off-shell.

B. VBFNLO

VBFNLO [40–42] is a flexible parton-level Monte-Carlo generator for processes with electroweak bosons. It allows the simulation of vector-boson fusion processes with the production of a Higgs boson or one or two massive gauge bosons as well as the production of two or three electroweak gauge bosons, including final states with photons. All these processes are implemented at next-to-leading order in the strong coupling constant. Furthermore, gluon-fusion production of Higgs plus two jets and of two electroweak bosons is implemented at the leading one-loop level. The program allows to place arbitrary cuts on the final-state particles and implements various scale choices. Any available PDF set can be used via a link to LHAPDF[43]. Events can be written out both in weighted and unweighted form and the LHE [44] as well as the HepMC [45] format.

All processes include fully leptonic decays of the gauge bosons, where the user can choose whether a particular final state is desired or all combinations, with or without the third generation, should be summed over and included in the event file. Off-shell effects including contributions from virtual photons instead of Z bosons are taken into account, while Pauli-interference effects for identical charged leptons are neglected. Furthermore, for the production of two massive gauge bosons, both direct and via vector-boson fusion, and the triboson process W^+W^-Z , semi-leptonic decays are available as well, where one boson decays into a quark pair, while the other ones still decay leptonically. Again either a specific flavor final state, only first- and second-generation quarks, or all light quarks including bottom quarks can be chosen. An extension to the other triboson processes is planned for the future.

Anomalous triple and quartic gauge couplings are implemented for all vector-boson-fusion processes with production of one or two gauge bosons, and all diboson and triboson processes [46, 47]. The operator structure has already been described in Section II. Note that the considered operators do not give any contributions to the diboson processes with two neutral particles in the final state, i.e. ZZ , $Z\gamma$ and $\gamma\gamma$. In all processes a form factor

$$F = \left(1 + \frac{s}{\Lambda}\right)^{-p} \quad (70)$$

can be applied to ensure unitarity at high energies [48–52]. Here s is a universal scale for each phase-space point, taken to be equal to the squared invariant mass of the produced bosons and Λ and p are free parameters describing the mass scale of the cut-off and the power of the damping, respectively. p should be chosen to be at least 1 for the dimension-6 and 2 for the dimension-8 operators to possess the required damping at high energies.

Additionally, a dedicated form factor tool can be downloaded from the VBFNLO web site [53]. The tool calculates on-shell VV scattering and computes the lowest ($J = 0$) contribution to the partial wave decomposition of the amplitude. The unitarity criterion is that the real part of this contribution must be below 0.5 [48]. We check each possible combination in $VV \rightarrow VV$ where $V = W, Z, \gamma$ separately as well as the combination of all channels with the same electrical charge of the VV system. After reading the anomalous coupling parameters from an input file, the output of the program then consists of the partonic center-of-mass energy for each channel where unitarity is first violated. This is performed both for the helicity combination giving the largest constraint and the most restrictive linear combination obtained by diagonalizing the T -matrix. Additionally, a value for Λ is calculated for each case that just ensures tree-level unitarity up to the given energy, taking the exponent p and the maximum considered energy set in the input file.

C. The event generator WHIZARD

WHIZARD [54] is a Monte Carlo event generator for hadron and lepton colliders. The most recent public version is 2.1.1, while an α release of the new version 2.2 will come out later this summer. WHIZARD contains the optimizing matrix element generator O’Mega [55]. O’Mega has been written in the functional language OCaml that allows for great versatility and flexibility. It uses the concept of directed acyclical graphs (DAGs) to generate amplitudes that are optimal in the sense that all redundancies due to common

subamplitudes and gauge invariance have been avoided. On top of that, a common subexpression elimination for equivalent flavor combinations is foreseen [56]. QCD quantum numbers are treated using the color flow formalism [57], that is ideally suited for transferring the color information to the parton shower (WHIZARD has its own k_T -ordered and analytic parton showers [58], but no hadronization). O'Mega supports all spins from scalars up to spin 3/2 [59] and tensor particles. A large library of vertex functions is supported for 3- and 4-point interactions as well as for higher-dimensional operators. Completely general Lorentz structures will be supported in the upcoming version, 2.2 [56]. WHIZARD is particularly specialized an beyond the SM (BSM) models, containing a large number of implemented models ranging from a variety of SUSY models, Little Higgs models, extra-dimensional models to models with anomalous couplings. An interface to the Lagrangian to Feynman rules converter FeynRules allows for the inclusion of basically arbitrary QFT-based BSM models [60]. Both O'Mega and WHIZARD have a large intrinsic testsuite that guarantees the inner consistency and prevents regressions during the development, e.g. there are Ward- and Slavnov-Taylor identities being checked [61].

Phase-space integration is performed by an adaptive multi-channel Monte-Carlo integration provided by the subpackage VAMP [62]. The new version of WHIZARD also contains alternative integration methods that are e.g. better suited for simple decay processes. The WHIZARD core that has been recasted in a very modern, modularized and object-oriented form in Fortran2003 steers the matrix element generation, compilation, phase space generation and interfacing to external libraries for PDFs, event formats, and hadronization. The input to WHIZARD happens through a universal scripting language SINDARIN, which is a very self-contained user-friendly syntax as input method to define processes, scales, cuts, and analyses. This input syntax allows to define arbitrary kinematical expressions for cuts and scales.

One of the main fields of WHIZARD applications (as in the context here) is for electroweak physics, particularly anomalous couplings and new resonances in the EW sector [17, 63, 64]. Other areas of applications not relevant in the context of the EW Snowmass White Paper (QCD, other BSM, ILC physics, etc.) are left out here for brevity.

D. The Role of Higher-order Corrections

Higher-order corrections play an important role for accurate predictions at the LHC. In this section we study the impact of NLO QCD corrections in vector-boson fusion and triboson processes and how they impact the extraction of anomalous quartic gauge couplings. As example of these two process classes we take the processes W^+W^+jj and $W^+\gamma\gamma$, respectively. The NLO results including anomalous QGCs presented in Sections III D 1 and III D 3 have been obtained with VBFNLO. We discuss the impact of a parton shower on the example of W^+W^+jj production with POWHEG+PYTHIA [65] in Section III D 2. Finally, in Section III D 4 we discuss the impact of NLO electroweak corrections in triboson processes.

1. Vector-boson-fusion process W^+W^+jj with VBFNLO

The production of a vector-boson pair via vector-boson fusion [66–70] has a characteristic signature of two high-energetic, so-called tagging jets in the forward region of the detector, which are defined as the two jets with the largest transverse momentum. This can be exploited experimentally by requiring that there is a large rapidity separation ($\Delta\eta_{jj} > 4$) between the tagging jets, they are in opposite detector hemispheres ($\eta_{j_1} \times \eta_{j_2} < 0$) and they possess a large invariant mass ($M_{jj} > 600$ GeV). Additional central jet radiation at higher orders is strongly suppressed due to the exchange of a color-singlet in the t-channel, in contrast to typical QCD-induced backgrounds. Higher-order corrections are typically small, below the 10% level, and reduce the residual scale uncertainty to about 2.5%. Choosing the momentum transfer between an incoming and an outgoing parton along a fermion line proves to be particularly advantageous, as then also corrections to important distributions are small and flat over the whole range.

As example we take the process $pp \rightarrow e^+\nu_e\mu^+\nu_\mu jj$ with anomalous coupling $\frac{f_{T,1}}{\Lambda^4} = 200 \text{ TeV}^{-4}$ and formfactor scale $\Lambda = 1188$ GeV and exponent $p = 4$. The results for the total cross sections at LO and NLO are shown in Tab. IV. Switching on the anomalous couplings increases the cross section by just under 20%,

	σ_{LO}	σ_{NLO}
SM	1.169 fb	1.176 fb
anom.coupl.	1.399 fb	1.388 fb

TABLE IV: Total cross sections at LO and NLO for the process $pp \rightarrow e^+ \nu_e \mu^+ \nu_\mu jj$ in the SM and with anomalous coupling $\frac{f_{T_1}}{\Lambda^4} = 200 \text{ TeV}^{-4}$. Statistical errors from Monte Carlo integration are below the per mille level.

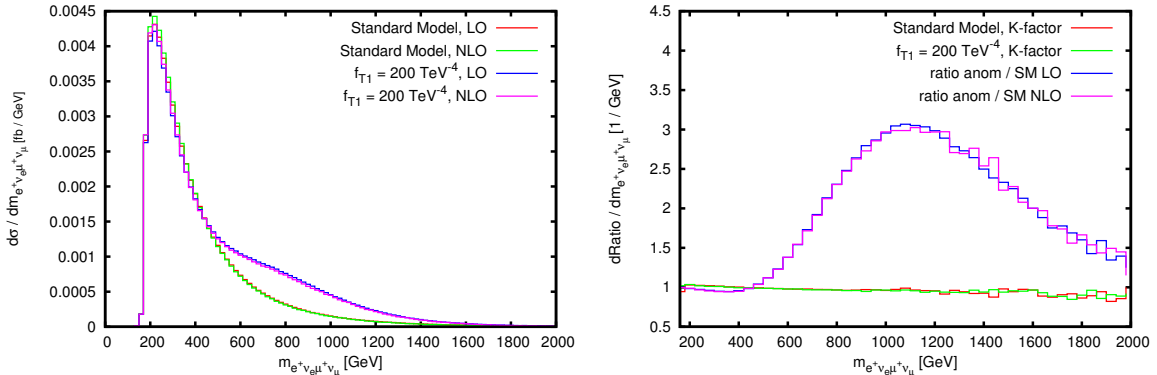


FIG. 2: Invariant-mass distribution of the two lepton, two neutrino system. *Left*: Differential cross section for the SM and with anomalous coupling T_1 at LO and NLO. *Right*: Differential K-factors for the SM and with anomalous coupling as well as the cross-section ratio between anomalous coupling and SM for LO and NLO.

and NLO QCD corrections hardly change this number. This can also be seen in Fig. 2 where we show the differential distribution with respect to the invariant mass of the two leptons and the two neutrinos. In the left-hand plot we present the differential cross section in the SM and with anomalous coupling switched on both at LO and NLO. Similar to the integrated cross section, the difference between LO and NLO is small in both cases. In contrast the anomalous couplings yield a positive contribution to the cross section over the SM, which starts at an invariant mass of about 500 GeV, before the formfactor, introduced to preserve unitarity, damps the contributions again at higher invariant masses. On the right-hand side we present two groups of ratios. The differential K factor is flat and close to one both for the SM and the anomalous coupling scenario. The second set shows the ratio of differential anomalous-coupling over SM cross section both at LO and NLO. The two curves agree well and show enhancements of the cross section up to a factor of three. Hence, in this process higher-order corrections do not influence the extraction of anomalous couplings.

2. Vector-boson-fusion process W^+W^+jj in the POWHEG BOX

NLO-QCD calculations are a crucial prerequisite for precision analyses at the LHC, reducing theoretical uncertainties associated with hard scattering processes significantly. On the other hand, a realistic description of the additional hadronic activity that occurs in any collider environment crucially relies on parton-shower Monte Carlo generators such as HERWIG [71] or PYTHIA [24]. The perturbative accuracy of these programs is, however, limited to leading logarithmic accuracy. The most realistic yet accurate predictions available to date for processes with many particles in the final state are thus obtained by combining NLO-QCD calculations for the hard scattering with parton shower programs, for example in the framework of the POWHEG formalism [72, 73]. Such a matching can be performed with the help of the POWHEG BOX [74], a repository that provides all process-independent building blocks of the matching procedure, while process-specific elements have to be provided by the user.

Building on existing NLO-QCD calculations [66, 69, 75, 76], recently various VBF processes have been implemented in the POWHEG BOX [65, 77–80]. The code developed is publicly available from the project

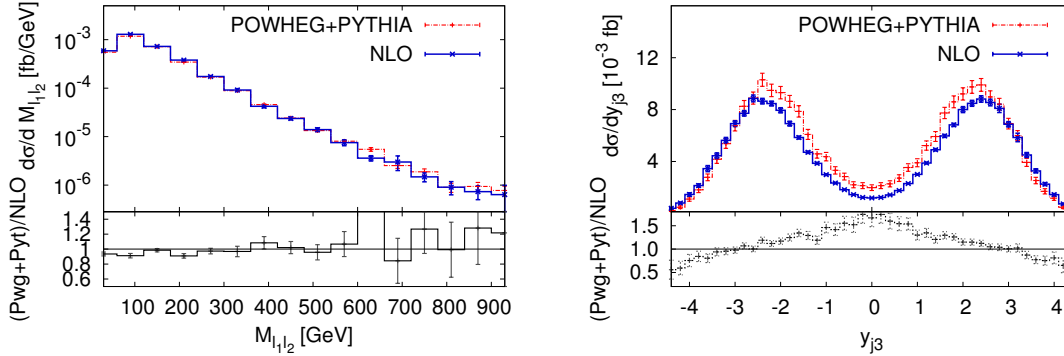


FIG. 3: Invariant mass distribution of the charged lepton pair (left) and rapidity distribution of the third jet (right) in VBF-induced $e^+\nu_e\mu^+\nu_\mu jj$ production at the LHC with $\sqrt{s} = 7$ TeV and the selection cuts described in the text. The lower panels show the respective ratios of the POWHEG+PYTHIA and the NLO-QCD results. Horizontal bars indicate statistical errors in each case.

webpage, <http://powhegbox.mib.infn.it/>, and can be tailored to the user's needs for any dedicated study. In order to assess the impact of parton-shower effects on NLO-QCD predictions for VBF-induced W^+W^+jj production at the LHC, numerical analyses for a representative setup have been performed for the $e^+\nu_e\mu^+\nu_\mu jj$ final state [65]. At a collision energy of $\sqrt{s} = 7$ TeV, the MSTW2008 parton distribution functions [81] are used for incoming protons and the FASTJET package [82] for the reconstruction of jets via the k_T algorithm with a resolution parameter of $R = 0.4$. Events are showered with PYTHIA 6.4.21, including hadronization corrections and underlying event with the Perugia 0 tune. At least two hard jets are required with $p_{T,j} \geq 20$ GeV and $|y_j| \leq 4.5$, well-separated from each other such that $|y_{j_1} - y_{j_2}| > 4$, $y_{j_1} \times y_{j_2} < 0$, and $M_{j_1 j_2} > 600$ GeV. In addition, an e^+ and a μ^+ with $p_{T,\ell} \geq 20$ GeV, $|y_\ell| \leq 2.5$, $\Delta R_{j\ell} \geq 0.4$, $\Delta R_{\ell\ell} \geq 0.1$, located between the two tagging jets, are requested. For the renormalization and factorization scales dynamical choices bound to the kinematics of the underlying Born configuration are made.

In this setup distributions related to the tagging jets or the hard leptons turn out to be rather insensitive to parton-shower effects. As illustrated by Fig. III D 2 (left panel) for the invariant mass distribution of the charged-lepton pair, the NLO-QCD and the POWHEG+PYTHIA results are very similar, both in normalization and shape. More pronounced effects of the parton shower occur in observables related to the emission of an extra hard jet, c.f. Fig. III D 2 (right panel) for $d\sigma/dy_{j_3}$. When the rapidity distribution of a third jet is used in order to estimate central-jet veto efficiencies this effect should be carefully taken into account.

3. Triboson process $W^+\gamma\gamma$ with VBFNLO

The second group of process where anomalous quartic gauge couplings can be tested are the triboson processes [83–93]. The quartic vertex enters via an s -channel vector boson, which decays into three vector bosons, while diagrams with two or three bosons attached to the quark line as well as non-resonant contributions form an irreducible background. These processes have been shown to possess quite large K factors, typically between 1.5 and 1.8, mostly due to the additional quark-gluon-induced production processes first entering in the real-emission process. They also have a considerable scale dependence. While the dependence on the factorization scale can be reduced by NLO QCD corrections, the strong coupling constant first enters in the real emission part and therefore shows a large variation with the scale.

The example process we are considering here is $pp \rightarrow e^+\nu_e\gamma\gamma$ [89, 90]. In this process the K factor with a numerical value of about 3 is particularly large. This is due to the fact that the SM amplitude vanishes when the two photons are collinear and $\cos\theta_W = \frac{1}{3}$, where θ_W is the angle between the W and the incoming quark in the partonic center-of-mass frame. This so-called radiation zero [94–96] is spoiled by the extra jet emission at NLO, therefore giving huge K factors in these phase-space regions. The numerical values for the

	σ_{LO}	σ_{NLO}
SM	1.124 fb	3.674 fb
anom.coupl.	1.216 fb	3.787 fb

TABLE V: Total cross sections at LO and NLO for the process $pp \rightarrow e^+ \nu_e \gamma \gamma$ in the SM and with anomalous coupling $\frac{f_{T_6}}{\Lambda^4} = 2000 \text{ TeV}^{-4}$. Statistical errors from Monte Carlo integration are below the per mille level.

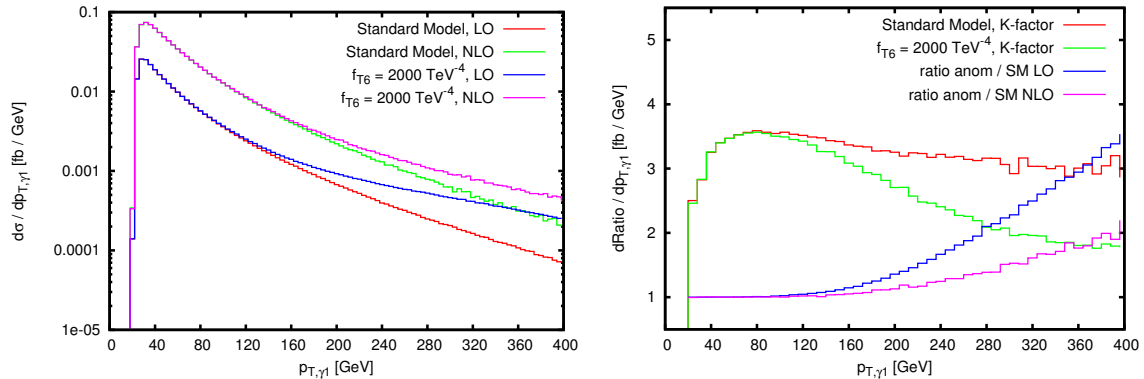


FIG. 4: Transverse-momentum distribution of the harder photon. *Left:* Differential cross section for the SM and with anomalous coupling T_6 at LO and NLO. *Right:* Differential K-factors for the SM and with anomalous coupling as well as the cross-section ratio between anomalous coupling and SM for LO and NLO.

integrated cross section are tabulated in Table V. As anomalous coupling we choose the operator T_6 with $\frac{f_{T_6}}{\Lambda^4} = 2000 \text{ TeV}^{-4}$, formfactor scale $\Lambda = 1606 \text{ GeV}$ and exponent $p = 4$.

Turning to differential distributions, we show the transverse momentum distribution of the harder photon in Figure 4. The left-hand side shows again the differential integrated cross section. Both the SM and the anomalous-coupling scenario show differential NLO cross sections which are significantly larger than their LO counterpart. Contributions from anomalous couplings start to contribute for transverse photon momenta above 100 GeV and their relative size becomes gradually larger when going to higher momenta as expected.

On the right-hand side one can see that the K-factor behavior differs for the SM and the anomalous coupling scenario. While, in the SM, the K factor is almost constant and only slightly decreases when going to larger transverse momenta, there is a much stronger decrease when anomalous couplings are switched on. At the high end of the shown range, the K factor has reached a value of around 1.8, which is the number typically observed in other triboson processes involving W s. As the effect of the anomalous coupling increases, the cancellation between different amplitudes gets gradually destroyed and the radiation zero filled up. Only the effects from additional jet radiation remain, yielding the smaller K factor.

That this is indeed the case can be seen in Fig. 5. Here we require additionally that the transverse momentum of the harder photon exceeds 200 GeV and the invariant mass of the lepton-neutrino system exceeds 75 GeV to suppress radiation off the final-state lepton. The effect of the radiation zero should be visible as a dip at zero in the rapidity difference between the diphoton system and the lepton-neutrino system, which can be indeed observed for the LO SM curve. In contrast the anomalous-coupling curve shows no such behavior even at LO, and at NLO the dip is filled in both cases.

Turning back to the right-hand plot of Fig. 4, the ratio between anomalous-coupling and SM prediction decreases when going from LO to NLO. This is due to the same effect, as part of the additional contribution is caused by filling up the radiation zero, which is no longer present at NLO because there already QCD effects have caused this. Hence, for this process group, higher-order corrections play an important role and cannot be neglected when determining the size of or limits on anomalous quartic gauge couplings.

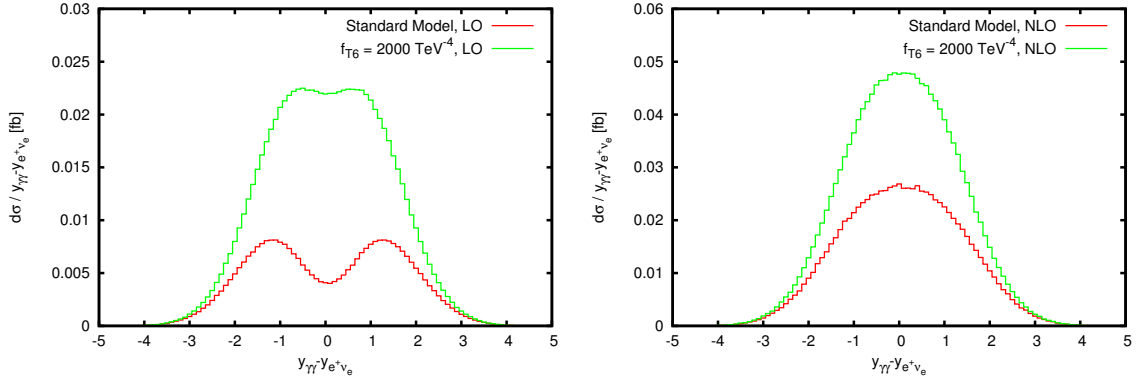


FIG. 5: Rapidity difference of the diphoton system and the lepton-neutrino system for the SM and the anomalous coupling scenario. *Left*: LO distributions *Right*: NLO distributions

4. Electroweak corrections to triboson processes

The first calculation of electroweak NLO corrections for a triboson process at hadron colliders has appeared only very recently. Hence, no publicly available Monte Carlo implementation is available at the present stage. For gauge boson pair production via vector-boson fusion electroweak corrections no results exist in the literature at the current stage.

In Ref. [97] the full NLO corrections to on-shell WWZ production have been considered. Besides the QCD corrections already calculated in Refs. [84, 86], additional virtual electroweak diagrams with loops up to the pentagon level appear as well as real-emission processes with an additional external photon. There, processes with both photon radiation and initial-state photons are taken into account. The latter appear when using PDFs with photons [98, 99]. Additionally, in this case the photon-initiated contribution of $\gamma\gamma \rightarrow WWZ$ is added at tree-level. The electroweak corrections are typically quite small for integrated cross sections, of about -2%. They can, however, get significant in differential distributions. For example, looking at the transverse-momentum distribution of the Z boson, at the 14 TeV LHC one observes corrections of up to -30% for transverse momenta of 1 TeV. Thereby, the photon-initiated processes play an important role to partly cancel large Sudakov virtual corrections.

IV. COMPARISON OF PREDICTIONS FOR MULTI-BOSON PRODUCTION WITH WHIZARD, VBFNLO AND MADGRAPH

Whenever more than one program is available to calculate the same quantity, it is an important cross-check to ensure that the theory predictions agree when choosing the same set of input parameters. Therefore we compare the predictions for the three programs MadGraph5, version 1.5.12, using the anomalous couplings implementation from Ref. [16], VBFNLO 2.7.0 beta 3 and WHIZARD 2.1.1. These three programs have been developed independently of each other, so agreement provides a strong cross-check. As process we have taken the same-sign W -pair vector-boson scattering process $pp \rightarrow e^+ \nu_e \mu^+ \nu_\mu jj$. We calculate this process at leading order for the LHC with a center-of-mass energy of 14 TeV using the CTEQ6L1 [100] pdf set with a fixed factorization scale $\mu = 2M_W$. No external bottom or top quarks are taken into account. The SM electro-weak input parameters are set to $M_W = 80.398$ GeV, $M_Z = 91.1876$ GeV, $M_H = 126$ GeV and $G_F = 1.16637 \cdot 10^{-5}$ GeV $^{-2}$ and the others fixed via electro-weak tree-level relations. The widths of the bosons are $\Gamma_W = 2.097673$ GeV, $\Gamma_Z = 2.508420$ GeV and $\Gamma_H = 4.277$ MeV. All fermions are taken as massless. Cuts on the final-state particles are as follows:

$$\begin{aligned}
 p_{T,\ell} &> 20 \text{ GeV} & |\eta_\ell| &< 2.5 \\
 p_{T,j} &> 30 \text{ GeV} & |\eta_j| &< 4.5 \\
 |\Delta\eta_{jj}| &> 4 & M_{jj} &> 600 \text{ GeV} .
 \end{aligned} \tag{71}$$

The VBFNLO program neglects any s-channel diagrams appearing, while for the other two codes these are included as well. Their numerical impact is, however, negligible due to the large invariant mass cut of the two jets. As anomalous quartic gauge couplings we take $f_{S,0} = f_{S,1} = \pm 10$ TeV $^{-4}$ in the VBFNLO and MadGraph5 scheme, which corresponds to $a_4 = \pm 4.59 \cdot 10^{-3}$ in WHIZARD. With these choices unitarity would get violated at 1.2 TeV. Due to the more technical nature of the comparison, and as there is no unitarization scheme supported commonly between all three programs, we do not take this into account further.

In Table VI we show results for the integrated cross section for the SM and both signs of the anomalous coupling choice. All three codes show a very good agreement with deviations of only a few per mill. Between VBFNLO and WHIZARD the level of agreement is compatible with statistical fluctuations from Monte Carlo integration, while the MadGraph5 result is slightly lower in all three cases. To verify that this is not due to a mismatch in the input parameters, we have compared the squared matrix element of the subprocess $uc \rightarrow e^+ \nu_e \mu^+ \nu_\mu ds$, which has no s-channel contributions, between MadGraph5 and VBFNLO for 100 randomly chosen phase-space points. Here we find excellent agreement at the sub-per mill level between the two codes.

In Fig. 6 we then compare differential distributions between MadGraph5, VBFNLO and WHIZARD. Each code has been asked to generate 1 million unweighted events, which form the input of each plot. The left column shows the invariant mass of the two jets, while in the right column the invariant mass of the two charged leptons is plotted. The top row presents each distribution for the SM, while in the middle and bottom row results for positive and negative anomalous couplings are shown, respectively. The lower part of each plot shows the differential cross section of each code compared to the weighted average of all three codes.

Similar to the integrated results, there is good agreement between all three codes. Deviations from the weighted average are compatible with those from finite event statistics, indicated by the error bars. No systematic shifts are visible, although MadGraph5 does tend to favor slightly smaller differential cross

	Standard Model	$f_{S,0} = f_{S,1} = +10$ TeV $^{-4}$	$f_{S,0} = f_{S,1} = -10$ TeV $^{-4}$
MadGraph5	1.3062(2) fb	1.7918 (2) fb	1.8295 (2) fb
VBFNLO	1.3098(4) fb	1.7932 (7) fb	1.8310 (7) fb
WHIZARD	1.3094(8) fb	1.7951(10) fb	1.8325(12) fb

TABLE VI: Integrated cross section for the process $pp \rightarrow e^+ \nu_e \mu^+ \nu_\mu jj$ with the cuts defined in Eq. 71. Results are given for all three programs for both the SM and both signs in the anomalous coupling choice.

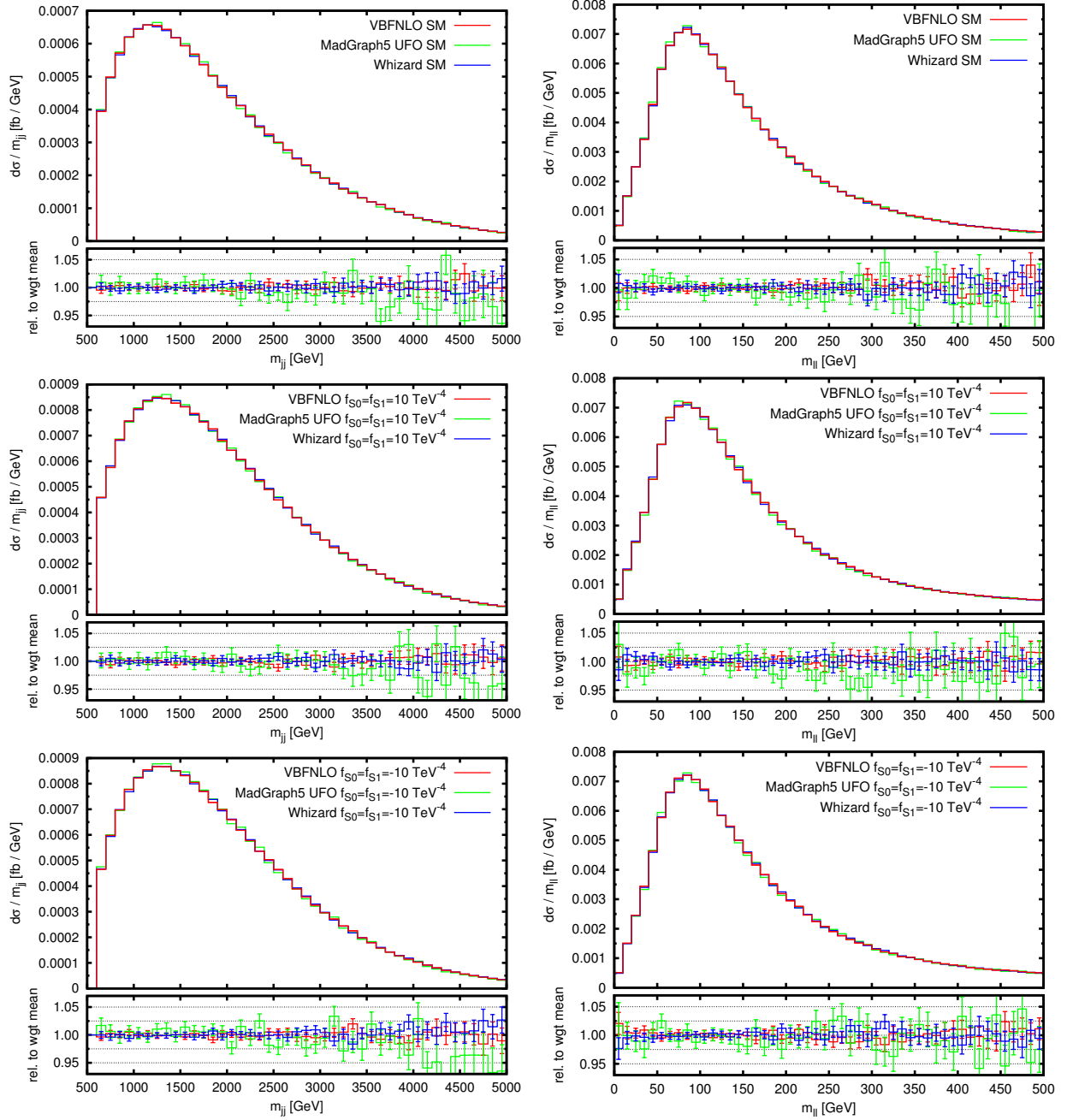


FIG. 6: Comparison of differential distributions between MadGraph5, VBFNLO and WHIZARD for the process $pp \rightarrow e^+ \nu_e \mu^+ \nu_\mu jj$. *Left*: Invariant mass of the two jets, *Right*: invariant mass of the two charged leptons. *Top*: SM, *Middle*: positive anomalous coupling, *Bottom*: negative anomalous coupling. The upper part of each plot shows the differential cross section, while the lower part shows the ratio of each code to the weighted mean of all three codes.

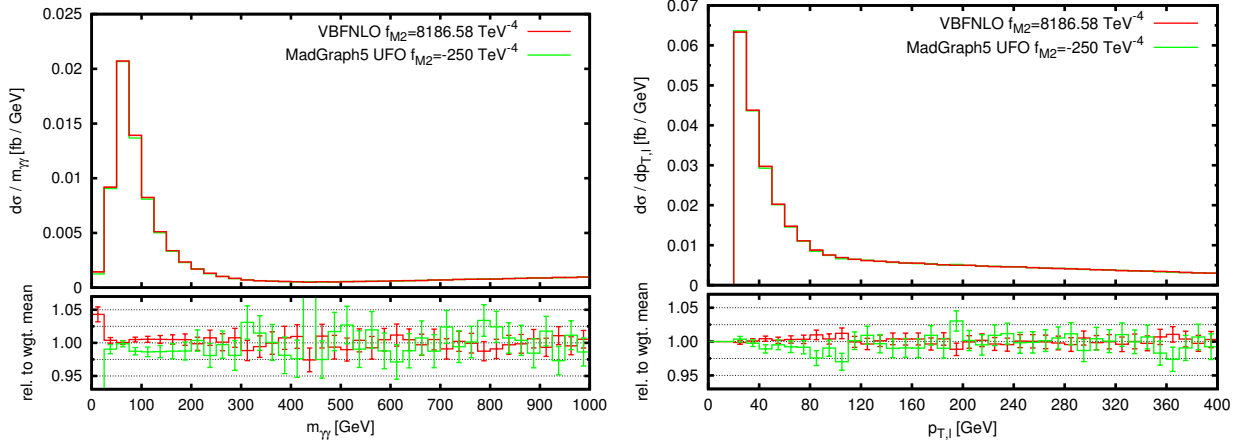


FIG. 7: Comparison of differential distributions between MadGraph5 and VBFNLO for the process $pp \rightarrow e^+ \nu_e \gamma \gamma$ using the anomalous quartic gauge coupling operator $M2$. *Left*: Invariant mass of the photon pair, *Right*: transverse momentum of the lepton.

sections in the large m_{jj} range. Comparing the two distributions between the SM and the two anomalous coupling scenarios, we see that the shape of the m_{jj} distribution hardly changes. The situation is different for the $m_{\ell\ell}$ distribution. Here we observe that for low invariant masses the distribution receives no additional contribution. This can for example be seen when looking at the bin with the largest differential cross section, whose height stays approximately the same. On the other hand, for larger invariant masses a significant increase of the differential cross section happens. Such a behavior is not surprising, as the invariant mass of the two leptons is directly related to the invariant mass of the WW system, and therefore one expects that the effects on anomalous couplings become larger for larger values, while no such link exists for the invariant mass of the two jets.

To further corroborate the agreement in the implementation of anomalous quartic gauge couplings, we have performed an additional cross-check between MadGraph5 and VBFNLO calculating the triboson process $pp \rightarrow e^+ \nu_e \gamma \gamma$. As anomalous quartic gauge coupling we choose the operator $M2$ with numerical value $f_{M2} = 8187 \text{ TeV}^{-4}$ in the VBFNLO and $f_{M2} = -250 \text{ TeV}^{-4}$ in the MadGraph5 convention. The integrated cross sections are $1.8012(8) \text{ fb}$ and $1.8172(5) \text{ fb}$ in the SM case and $4.2482(19) \text{ fb}$ and $4.2660(13) \text{ fb}$ including the anomalous quartic gauge coupling, where the first value in both cases refers to MadGraph5 and the second one to VBFNLO, respectively. While some difference exceeding the statistical errors from Monte Carlo integration is also present here, the agreement is at the sub-percent level for both scenarios and hence good.

In Fig. 7 we show the differential cross section for the invariant mass of the photon pair on the left-hand side and for the transverse momentum of the lepton on the right-hand side. In both cases we observe a reasonable agreement between the two codes within statistical errors. We have also checked several other distributions and do not see any deviations that would be incompatible with an explanation by statistical effects.

V. SUMMARY

In this Snowmass 2013 white paper we presented an overview of the theory of electroweak non-standard interactions and of publicly available Monte Carlo tools that provide predictions for electroweak vector boson pair and triple production as well as vector boson scattering at the LHC, including non-standard EW interactions. We reviewed the role of higher-order corrections in the study of non-standard EW couplings in these processes, using VBFNLO and a POWHEG BOX implementation of higher-order QCD corrections to $WWjj$ production. We performed a tuned comparison of predictions obtained with MadGraph5, VBFNLO, and WHIZARD for a number of relevant observables at leading order QCD and including higher-dimension operators in EFT, and found good agreement.

Acknowledgments

C. D. is supported in part by the U. S. Department of Energy under Contract No. DE-FG02-13ER42001. B. F. and M. R. would like to thank D. Zeppenfeld for many helpful and stimulating discussions. B. F. and M. R. acknowledge support by the BMBF under Grant No. 05H09VKG (“Verbundprojekt HEP-Theorie”). B. J. would like to thank the Research Center Elementary Forces and Mathematical Foundations (EMG) of the Johannes Gutenberg University Mainz. O. M. is a fellow of the Belgian American Educational Foundation and a chercheur logistique post-doctoral from F.R.S-FNRS. His work is partially supported by the IISN MadGraph convention 4.4511.10. The work of D. W. is supported in part by the U.S. National Science Foundation under grant no. PHY-1118138.

-
- [1] J. Reuter, W. Kilian and M. Sekulla, arXiv:1307.8170 [hep-ph].
- [2] B. Grzadkowski, M. Iskrzynski, M. Misiak and J. Rosiek, JHEP **1010**, 085 (2010) [arXiv:1008.4884 [hep-ph]].
- [3] C. Arzt, M. B. Einhorn and J. Wudka, Nucl. Phys. B **433**, 41 (1995) [hep-ph/9405214].
- [4] O. J. P. Eboli, M. C. Gonzalez-Garcia and J. K. Mizukoshi, Phys. Rev. D **74**, 073005 (2006) [hep-ph/0606118].
- [5] See, for instance, J. Bagger, S. Dawson and G. Valencia, Nucl. Phys. B **399**, 364 (1993) [hep-ph/9204211].
- [6] A. S. Belyaev, O. J. P. Eboli, M. C. Gonzalez-Garcia, J. K. Mizukoshi, S. F. Novaes and I. Zacharov, Phys. Rev. D **59**, 015022 (1999) [hep-ph/9805229];
- [7] O. J. P. Eboli, M. C. Gonzalez-Garcia, S. M. Lietti and S. F. Novaes, Phys. Rev. D **63**, 075008 (2001) [hep-ph/0009262].
- [8] O. J. P. Eboli, M. C. Gonzalez-Garcia and S. M. Lietti, Phys. Rev. D **69**, 095005 (2004) [hep-ph/0310141].
- [9] K. Hagiwara, R. D. Peccei, D. Zeppenfeld and K. Hikasa, Nucl. Phys. B **282**, 253 (1987).
- [10] K. Hagiwara, S. Ishihara, R. Szalapski and D. Zeppenfeld, Phys. Rev. D **48**, 2182 (1993).
- [11] J. Wudka, Int. J. Mod. Phys. A **9**, 2301 (1994) [hep-ph/9406205].
- [12] See for instance, and references therein, <http://pdg.lbl.gov/2010/reviews/rpp2010-rev-wz-quartic-couplings.pdf>.
- [13] W. J. Stirling and A. Werthenbach, Eur. Phys. J. C **14**, 103 (2000) [hep-ph/9903315].
- [14] G. Belanger and F. Boudjema, Phys. Lett. B **288**, 201 (1992).
- [15] O. J. P. Eboli, M. C. Gonzalez-Garcia and S. F. Novaes, Nucl. Phys. B **411**, 381 (1994) [hep-ph/9306306].
- [16] <http://feynrules.irmp.ucl.ac.be/wiki/AnomalousGaugeCoupling>
- [17] A. Alboteanu, W. Kilian and J. Reuter, JHEP **0811** (2008) 010 [arXiv:0806.4145 [hep-ph]].
- [18] C. Degrande, N. Greiner, W. Kilian, O. Mattelaer, H. Mebane, T. Stelzer, S. Willenbrock and C. Zhang, arXiv:1205.4231 [hep-ph].
- [19] J. Alwall, M. Herquet, F. Maltoni, O. Mattelaer and T. Stelzer, JHEP **1106**, 128 (2011) [arXiv:1106.0522 [hep-ph]].
- [20] V. Hirschi, R. Frederix, S. Frixione, M. V. Garzelli, F. Maltoni and R. Pittau, JHEP **1105**, 044 (2011) [arXiv:1103.0621 [hep-ph]].
- [21] P. Artoisenet, V. Lemaître, F. Maltoni and O. Mattelaer, JHEP **1012**, 068 (2010) [arXiv:1007.3300 [hep-ph]].
- [22] R. Frederix, S. Frixione, F. Maltoni and T. Stelzer, JHEP **0910**, 003 (2009) [arXiv:0908.4272 [hep-ph]].
- [23] F. Maltoni and T. Stelzer, JHEP **0302**, 027 (2003) [hep-ph/0208156].
- [24] T. Sjöstrand, S. Mrenna, P. Z. Skands, JHEP **0605** (2006) 026. [hep-ph/0603175].
- [25] S. Catani, F. Krauss, R. Kuhn and B. R. Webber, JHEP **0111**, 063 (2001) [hep-ph/0109231].
- [26] J. Alwall, S. Hoche, F. Krauss, N. Lavesson, L. Lomblad, F. Maltoni, M. L. Mangano and M. Moretti *et al.*, Eur. Phys. J. C **53**, 473 (2008) [arXiv:0706.2569 [hep-ph]].
- [27] A. Alwall, R. Frederix, S. Frixione, V. Hirschi, F. Maltoni, O. Mattelaer, P. Torrielli and M. Zaro, *In preparation*
- [28] C. Degrande, C. Duhr, B. Fuks, D. Grellscheid, O. Mattelaer and T. Reiter, Comput. Phys. Commun. **183**, 1201 (2012) [arXiv:1108.2040 [hep-ph]].
- [29] P. de Aquino, W. Link, F. Maltoni, O. Mattelaer and T. Stelzer, Comput. Phys. Commun. **183**, 2254 (2012) [arXiv:1108.2041 [hep-ph]].
- [30] H. Murayama, I. Watanabe and K. Hagiwara, KEK-91-11.
- [31] N. D. Christensen, P. de Aquino, N. Deutschmann, C. Duhr, B. Fuks, C. Garcia-Cely, O. Mattelaer and K. Mawatari *et al.*, arXiv:1308.1668 [hep-ph].
- [32] N. D. Christensen and C. Duhr, Comput. Phys. Commun. **180**, 1614 (2009) [arXiv:0806.4194 [hep-ph]].
- [33] N. D. Christensen, P. de Aquino, C. Degrande, C. Duhr, B. Fuks, M. Herquet, F. Maltoni and S. Schumann, Eur. Phys. J. C **71**, 1541 (2011) [arXiv:0906.2474 [hep-ph]].
- [34] F. Staub, Computer Physics Communications **184**, pp. 1792 (2013) [Comput. Phys. Commun. **184**, 1792 (2013)] [arXiv:1207.0906 [hep-ph]].
- [35] A. Semenov, Comput. Phys. Commun. **180**, 431 (2009) [arXiv:0805.0555 [hep-ph]].
- [36] C. Degrande, *In preparation*
- [37] P. Artoisenet, R. Frederix, O. Mattelaer and R. Rietkerk, JHEP **1303**, 015 (2013) [arXiv:1212.3460 [hep-ph]].
- [38] E. Conte, B. Fuks and G. Serret, Comput. Phys. Commun. **184**, 222 (2013) [arXiv:1206.1599 [hep-ph]].
- [39] J. de Favereau, C. Delaere, P. Demin, A. Giammanco, V. Lemaître, A. Mertens and M. Selvaggi, arXiv:1307.6346 [hep-ex].
- [40] K. Arnold, J. Bellm, G. Bozzi, F. Campanario, C. Englert, et al., *Release Note – VBFNLO-2.6.0*, arXiv:1207.4975 [hep-ph].
- [41] K. Arnold, J. Bellm, G. Bozzi, M. Brieg, F. Campanario, et al., *VBFNLO: A parton level Monte Carlo for processes with electroweak bosons – Manual for Version 2.5.0*, arXiv:1107.4038 [hep-ph].

- [42] K. Arnold et al., *VBFNLO: A parton level Monte Carlo for processes with electroweak bosons*, Comput. Phys. Commun. **180** (2009) 1661–1670, [arXiv:0811.4559](#) [hep-ph].
- [43] M. R. Whalley, D. Bourilkov and R. C. Group, hep-ph/0508110.
- [44] J. Alwall, A. Ballestrero, P. Bartalini, S. Belov, E. Boos, A. Buckley, J. M. Butterworth and L. Dudko *et al.*, Comput. Phys. Commun. **176**, 300 (2007) [hep-ph/0609017].
- [45] M. Dobbs and J. B. Hansen, Comput. Phys. Commun. **134**, 41 (2001).
- [46] B. Feigl, Diploma Thesis, ITP Karlsruhe 2009, <http://www.itp.kit.edu/diplomatheses.en.shtml>.
- [47] O. Schlimpert, Diploma Thesis, ITP Karlsruhe 2013, <http://www.itp.kit.edu/diplomatheses.en.shtml>.
- [48] V. D. Barger, K. -m. Cheung, T. Han and R. J. N. Phillips, Phys. Rev. D **42**, 3052 (1990).
- [49] U. Baur and D. Zeppenfeld, Phys. Lett. B **201**, 383 (1988).
- [50] U. Baur and D. Zeppenfeld, Nucl. Phys. B **308**, 127 (1988).
- [51] G. J. Gounaris, J. Layssac and F. M. Renard, Phys. Lett. B **332**, 146 (1994) [hep-ph/9311370].
- [52] G. J. Gounaris, J. Layssac, J. E. Paschalis and F. M. Renard, Z. Phys. C **66**, 619 (1995) [hep-ph/9409260].
- [53] <http://www.itp.kit.edu/vbfnloweb/wiki/doku.php?id=download:formfactor>
- [54] W. Kilian, T. Ohl and J. Reuter, Eur. Phys. J. C **71**, 1742 (2011) [arXiv:0708.4233 [hep-ph]].
- [55] M. Moretti, T. Ohl and J. Reuter, In *2nd ECFA/DESY Study 1998-2001* 1981-2009 [hep-ph/0102195].
- [56] W. Kilian, T. Ohl, J. Reuter, C. Speckner, in preparation.
- [57] W. Kilian, T. Ohl, J. Reuter and C. Speckner, JHEP **1210**, 022 (2012) [arXiv:1206.3700 [hep-ph]].
- [58] W. Kilian, J. Reuter, S. Schmidt and D. Wiesler, JHEP **1204**, 013 (2012) [arXiv:1112.1039 [hep-ph]].
- [59] J. Reuter, hep-th/0212154.
- [60] N. D. Christensen, C. Duhr, B. Fuks, J. Reuter and C. Speckner, Eur. Phys. J. C **72**, 1990 (2012) [arXiv:1010.3251 [hep-ph]].
- [61] T. Ohl and J. Reuter, Eur. Phys. J. C **30**, 525 (2003) [hep-th/0212224].
- [62] T. Ohl, Comput. Phys. Commun. **120**, 13 (1999) [hep-ph/9806432].
- [63] M. Beyer, W. Kilian, P. Krstonsic, K. Monig, J. Reuter, E. Schmidt and H. Schroder, Eur. Phys. J. C **48**, 353 (2006) [hep-ph/0604048].
- [64] W. Kilian, J. Reuter, M. Sekulla, in preparation.
- [65] B. Jäger and G. Zanderighi, JHEP **1111** (2011) 055 [arXiv:1108.0864 [hep-ph]].
- [66] B. Jager, C. Oleari and D. Zeppenfeld, JHEP **0607**, 015 (2006) [hep-ph/0603177].
- [67] B. Jager, C. Oleari and D. Zeppenfeld, Phys. Rev. D **73**, 113006 (2006) [hep-ph/0604200].
- [68] G. Bozzi, B. Jager, C. Oleari and D. Zeppenfeld, Phys. Rev. D **75**, 073004 (2007) [hep-ph/0701105].
- [69] B. Jager, C. Oleari and D. Zeppenfeld, Phys. Rev. D **80**, 034022 (2009) [arXiv:0907.0580 [hep-ph]].
- [70] A. Denner, L. Hosekova and S. Kallweit, Phys. Rev. D **86** (2012) 114014 [arXiv:1209.2389 [hep-ph]].
- [71] G. Corcella *et al.*, JHEP **0101** (2001) 010. [hep-ph/0011363].
- [72] P. Nason, JHEP **0411** (2004) 040. [hep-ph/0409146].
- [73] S. Frixione, P. Nason, C. Oleari, JHEP **0711** (2007) 070. [arXiv:0709.2092 [hep-ph]].
- [74] S. Alioli, P. Nason, C. Oleari, E. Re, JHEP **1006** (2010) 043. [arXiv:1002.2581 [hep-ph]].
- [75] T. Figy, C. Oleari and D. Zeppenfeld, Phys. Rev. D **68** (2003) 073005 [hep-ph/0306109].
- [76] C. Oleari and D. Zeppenfeld, Phys. Rev. D **69** (2004) 093004 [hep-ph/0310156].
- [77] P. Nason and C. Oleari, JHEP **1002** (2010) 037 [arXiv:0911.5299 [hep-ph]].
- [78] B. Jäger, S. Schneider and G. Zanderighi, JHEP **1209** (2012) 083 [arXiv:1207.2626 [hep-ph]].
- [79] F. Schissler and D. Zeppenfeld, JHEP **04** (2013) 057 [JHEP **1304** (2013) 057] [arXiv:1302.2884 [hep-ph]].
- [80] B. Jäger and G. Zanderighi, JHEP **1304** (2013) 024 [arXiv:1301.1695 [hep-ph]].
- [81] A. D. Martin, W. J. Stirling, R. S. Thorne, G. Watt, Eur. Phys. J. **C63** (2009) 189-285. [arXiv:0901.0002 [hep-ph]].
- [82] M. Cacciari, G. P. Salam, Phys. Lett. **B641** (2006) 57. [hep-ph/0512210].
- [83] A. Lazopoulos, K. Melnikov and F. Petriello, Phys. Rev. D **76**, 014001 (2007) [hep-ph/0703273].
- [84] V. Hankele and D. Zeppenfeld, Phys. Lett. B **661**, 103 (2008) [arXiv:0712.3544 [hep-ph]].
- [85] F. Campanario, V. Hankele, C. Oleari, S. Prestel and D. Zeppenfeld, Phys. Rev. D **78**, 094012 (2008) [arXiv:0809.0790 [hep-ph]].
- [86] T. Binoth, G. Ossola, C. G. Papadopoulos and R. Pittau, JHEP **0806**, 082 (2008) [arXiv:0804.0350 [hep-ph]].
- [87] G. Bozzi, F. Campanario, V. Hankele and D. Zeppenfeld, Phys. Rev. D **81**, 094030 (2010) [arXiv:0911.0438 [hep-ph]].
- [88] G. Bozzi, F. Campanario, M. Rauch, H. Rzehak and D. Zeppenfeld, Phys. Lett. B **696**, 380 (2011) [arXiv:1011.2206 [hep-ph]].
- [89] U. Baur, D. Wackerroth and M. M. Weber, PoS RADCOR **2009**, 067 (2010) [arXiv:1001.2688 [hep-ph]].
- [90] G. Bozzi, F. Campanario, M. Rauch and D. Zeppenfeld, Phys. Rev. D **83**, 114035 (2011) [arXiv:1103.4613 [hep-ph]].

- [91] G. Bozzi, F. Campanario, M. Rauch and D. Zeppenfeld, Phys. Rev. D **84**, 074028 (2011) [arXiv:1107.3149 [hep-ph]].
- [92] G. Bozzi, F. Campanario, C. Englert, M. Rauch, M. Spannoswky and D. Zeppenfeld, arXiv:1205.2506 [hep-ph].
- [93] J. M. Campbell, H. B. Hartanto and C. Williams, JHEP **1211**, 162 (2012) [arXiv:1208.0566 [hep-ph]].
- [94] R. W. Brown, K. L. Kowalski and S. J. Brodsky, Phys. Rev. D **28**, 624 (1983).
- [95] U. Baur, T. Han and J. Ohnemus, Phys. Rev. D **48**, 5140 (1993) [hep-ph/9305314].
- [96] U. Baur, T. Han, N. Kauer, R. Sobey and D. Zeppenfeld, Phys. Rev. D **56**, 140 (1997) [hep-ph/9702364].
- [97] D. T. Nhung, L. D. Ninh and M. M. Weber, arXiv:1307.7403 [hep-ph].
- [98] A. D. Martin, R. G. Roberts, W. J. Stirling and R. S. Thorne, Eur. Phys. J. C **39**, 155 (2005) [hep-ph/0411040].
- [99] R. D. Ball *et al.* [The NNPDF Collaboration], arXiv:1308.0598 [hep-ph].
- [100] J. Pumplin, D. R. Stump, J. Huston, H. L. Lai, P. M. Nadolsky and W. K. Tung, JHEP **0207**, 012 (2002) [hep-ph/0201195].